
Heterogeneous Ordinal Structure Learning with Bayesian Nonparametric Complexity Discovery

Amir Rafe, Ph.D.
Texas State University
San Marcos, USA
amir.rafe@txstate.edu
ORCID: 0000-0002-4089-2088

Subasish Das, Ph.D.
Texas State University
San Marcos, USA
subasish@txstate.edu
ORCID: 0000-0002-1671-2753

Abstract

Public attitudes toward artificial intelligence are heterogeneous, ordinally measured, and poorly captured by any single dependency graph. Existing ordinal structure learners assume a shared directed acyclic graph (DAG) across all respondents; recent heterogeneous ordinal graphical-model approaches focus on subgroup discovery rather than confirmatory cluster-specific DAG estimation; and latent profile analyses discard dependency structure entirely. We introduce a heterogeneous ordinal structure-learning framework combining monotone Gaussian score embedding, Bayesian nonparametric (BNP) complexity discovery via a truncated stick-breaking prior, and confirmatory fixed- K estimation with cluster-specific sparse DAG learning. The key methodological insight is a discovery-to-confirmation workflow: the nonparametric stage calibrates plausible archetype complexity, while inner-validated confirmatory refitting yields stable, interpretable structural estimates. On the 2024 Pew American Trends Panel AI attitudes survey, Wave 152 (W152) survey, ($N=4,788$, 8 ordinal items), the confirmatory $K^*=5$ model reduces holdout transformed-score mean squared error (MSE) by 25.8% over a single-graph baseline and by 4.6% over mixture-only clustering. A controlled tiered semi-synthetic benchmark calibrated to W152 structure validates recovery across difficulty regimes and transparently reveals failure modes under stress conditions.

1 Introduction

Public attitudes toward artificial intelligence are increasingly measured through large-scale ordinal survey batteries [Pew Research Center, 2024, Zhang and Dafoe, 2019, Scantamburlo et al., 2025]. Standard analyses typically make two simplifying assumptions: the population shares one dependency structure, and ordinal responses can be treated as continuous without distortion. Both are questionable. If subpopulations differ in how trust, regulation, and perceived benefits interact, a single shared graph mischaracterizes every group. This concern is substantive as well as statistical. Recent measurement work argues that AI attitudes contain separable positive and negative dimensions, with trust-related beliefs and institutional confidence varying in ways that do not collapse cleanly to a single pro-versus-anti axis [Schepman and Rodway, 2020, 2023, Zhang and Dafoe, 2019, Scantamburlo et al., 2025]. In exactly this setting, averaging respondents into one population graph risks obscuring the heterogeneity that survey researchers care about most.

Adjacent methodological literatures each address only part of this problem. Ordinal-aware Bayesian network (BN) methods respect category ordering but learn one shared graph [Luo et al., 2021, Grzegorzcyk, 2024, Ni et al., 2025]. Mixed graphical and psychometric network models estimate dependence among mixed or ordinal variables, but are typically undirected and fitted at the population level [Lee and Hastie, 2015, Epskamp et al., 2018]. Model-based clustering and latent profile analysis support subgroup discovery in respondent-level distributions, yet focus on profile recovery rather

than cluster-specific dependency structure [Fraley and Raftery, 2002, Shum and Lau, 2024]. Mixture-of-DAG models allow subgroup-specific structure but usually operate on continuous or categorical observations [Thiesson, 1997, Saeed et al., 2020, Castelletti and Consonni, 2023, Castelletti and Ferrini, 2024]. Recent heterogeneous ordinal or categorical graphical-model work moves closer to the present setting [Wang et al., 2025, Ferrini and Castelletti, 2026]. What remains useful here is a stable workflow for learning heterogeneous ordinal structure and reporting it defensibly.

We therefore study a three-stage framework: (i) a monotone Gaussian score embedding for ordinal data (§2.1), (ii) BNP complexity discovery via a truncated stick-breaking Dirichlet process (DP) mixture [Ferguson, 1973, Sethuraman, 1994] (§2.3), and (iii) confirmatory fixed- K heterogeneous structure estimation with cluster-specific sparse DAGs (§2.4). The core methodological idea is *discovery to confirmation*: use the nonparametric stage to learn plausible complexity, then report an inner-validated fixed-dimensional estimator rather than either arbitrary segmentation or the raw nonparametric fit. This design is more defensible for empirical reporting because the discovery stage calibrates complexity while the confirmatory stage yields a stable model for comparison and substantive interpretation.

We organize the empirical study around four research questions. **RQ1** (Complexity Discovery): How many latent archetypes does the data support, and does nonparametric discovery agree with inner-validated model selection? **RQ2** (Archetype Structure): Do the discovered archetypes exhibit qualitatively distinct dependency graphs, or do they differ only in mean profiles? **RQ3** (Model Comparison): Does the heterogeneous ordinal model improve holdout transformed-score prediction relative to single-graph and mixture-only baselines? **RQ4** (Validation): Can the framework recover known structure in controlled semi-synthetic data, and is it robust to prior specification and item-set perturbation? We evaluate the method on the 2024 Pew American Trends Panel (ATP) W152, a nationally representative U.S. survey on AI attitudes, using an analytic sample of $N=4,788$ respondents and 8 ordinal items.

The paper makes three contributions. First, it extends ordinal structure learning to subgroup-specific sparse DAGs through a heterogeneous workflow combining monotone score embedding and cluster-specific graphs. Second, it introduces a discovery-to-confirmation strategy that uses the BNP stage to calibrate complexity and an inner-validated fixed- K refit for reporting. Third, it shows on Pew W152 and a controlled benchmark that the approach recovers interpretable archetypes, improves fit over strong baselines, and makes its stability limits explicit.

2 Method

We present a heterogeneous ordinal structure-learning framework whose three-stage pipeline, ordinal embedding (§2.1), BNP complexity discovery (§2.3), and confirmatory fixed- K estimation (§2.4), is built on a cluster-specific structural model described in §2.2. Figure 1 provides an overview.

2.1 Monotone Gaussian Score Embedding

Let respondent $i = 1, \dots, N$ answer J ordinal items with $Y_{ij} \in \{1, \dots, C_j\}$. Ordinal responses cannot be treated as continuous without distorting dependency estimation. We embed each item into a monotone Gaussian score that preserves category ordering while enabling sparse Gaussian DAG estimation.

For item j , let $p_{jc} = P(Y_j = c)$ denote the empirical category mass. Define the cumulative midpoint:

$$u_{jc} = \sum_{\ell < c} p_{j\ell} + \frac{1}{2} p_{jc}, \quad (1)$$

and the category score:

$$s_j(c) = \Phi^{-1}(u_{jc}), \quad (2)$$

where Φ^{-1} is the standard normal quantile function. Each respondent’s observed ordinal value is then replaced by its category score:

$$X_{ij} = s_j(Y_{ij}), \quad (3)$$

and all subsequent structure learning operates on the transformed matrix $\mathbf{X} \in \mathbb{R}^{N \times J}$.

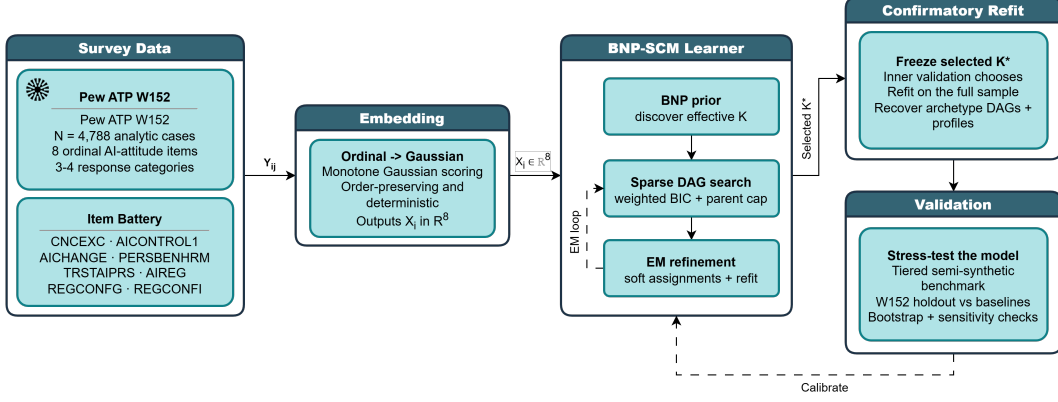


Figure 1: **Discovery-to-confirmation pipeline.** Ordinal survey responses are embedded via monotone Gaussian scoring, then a BNP mixture discovers plausible archetype complexity. Inner validation selects K^* , and a confirmatory refit produces stable archetype DAGs and profiles for substantive reporting.

This embedding is monotone ($c_1 < c_2 \Rightarrow s_j(c_1) < s_j(c_2)$), deterministic (unlike ordinal probit data augmentation [Albert and Chib, 1993]), and produces approximately standard-normal marginals. It preserves Spearman rank correlations exactly and avoids the computational cost of Markov chain Monte Carlo (MCMC)-based latent-variable models while respecting ordinal structure.

2.2 Archetype-Specific Structural Model

Let $z_i \in \{1, \dots, K\}$ denote respondent i 's latent archetype. Conditional on archetype k , the transformed item vector $\mathbf{X}_i = (X_{i1}, \dots, X_{iJ})^\top$ follows a sparse linear-Gaussian DAG:

$$X_{ij} = \beta_{k0,j} + \sum_{m \in \text{Pa}_k(j)} \beta_{km \rightarrow j} X_{im} + \varepsilon_{ijk}, \quad \varepsilon_{ijk} \sim \mathcal{N}(0, \sigma_{kj}^2), \quad (4)$$

where G_k is the directed acyclic graph for archetype k , $\text{Pa}_k(j)$ is the parent set of node j in G_k , $\beta_{km \rightarrow j}$ is the edge weight from node m to node j , and σ_{kj}^2 is the residual variance. Crucially, each archetype has its own adjacency matrix, parent sets, regression coefficients, and residual variances.

Cluster-specific Bayesian information criterion (BIC) scoring. For a given cluster k with soft responsibilities r_{ik} , the local weighted BIC for node j is:

$$\text{BIC}_{kj}(G_k) = n_k \log \left(\frac{\text{RSS}_{kj}}{n_k} \right) + d_{kj} \log n_k, \quad (5)$$

where $n_k = \sum_i r_{ik}$ is the effective cluster mass, $\text{RSS}_{kj} = \sum_i r_{ik} (X_{ij} - \hat{X}_{ij})^2$ is the responsibility-weighted residual sum of squares, and d_{kj} is the number of regression coefficients including the intercept. The graph-level objective is:

$$\text{BIC}_k(G_k) = \sum_{j=1}^J \text{BIC}_{kj}(G_k). \quad (6)$$

Graph search uses greedy acyclicity-constrained edge operations (add, delete, reverse) under a maximum-parent cap [Chickering, 2002].

2.3 Bayesian Nonparametric Complexity Discovery

The number of archetypes K should be learned from data rather than specified a priori. We use a truncated stick-breaking representation of a DP mixture [Sethuraman, 1994]:

$$V_k \sim \text{Beta}(1, \alpha), \quad \pi_k = V_k \prod_{\ell < k} (1 - V_\ell), \quad k = 1, \dots, K_{\max}, \quad (7)$$

where $\alpha > 0$ is the concentration parameter and K_{\max} is a finite truncation level. This stage discovers plausible archetype complexity by fitting the full mixture-of-DAGs model and observing how many components receive non-negligible mass.

Iterative soft-assignment refinement. The heterogeneous estimator alternates between responsibility updates (E-step) and responsibility-weighted DAG fitting (M-step) [Dempster et al., 1977]:

E-step. Update responsibilities using the current parameters:

$$r_{ik}^{(t+1)} \propto \tilde{\pi}_k^{(t)} \cdot p(\mathbf{X}_i | G_k^{(t)}, \theta_k^{(t)}), \quad (8)$$

where the smoothed cluster weights are:

$$\tilde{\pi}_k^{(t)} = \frac{\sum_i r_{ik}^{(t)} + \alpha/K}{N + \alpha}, \quad (9)$$

followed by row normalization over k .

M-step. For each cluster k , refit the cluster-specific DAG using the updated responsibilities:

$$(G_k^{(t+1)}, \theta_k^{(t+1)}) = \arg \max_{G, \theta} \sum_i r_{ik}^{(t+1)} \log p(\mathbf{X}_i | G, \theta) - \lambda \text{pen}(G), \quad (10)$$

where $\text{pen}(G)$ is the BIC complexity term from Eq. 5 and $\lambda=1$ throughout. Because greedy DAG search does not guarantee a global optimum, this constitutes a generalized expectation-maximization (EM) procedure. The refinement loop terminates when both the assignment-change rate and the objective change fall below a convergence threshold (see Appendix B).

2.4 Confirmatory Fixed- K Estimation

The BNP discovery stage provides a data-driven estimate of archetype complexity, but the non-parametric fit may over-split in practice (see §4.4). For stable empirical reporting, we select the confirmatory complexity via inner validation:

$$K^* = \arg \min_{K \in \mathcal{K}_{\text{grid}}} \text{MSE}_{\text{val}}(K), \quad (11)$$

where $\mathcal{K}_{\text{grid}} = \{2, 3, 4, 5, 6\}$ and the transformed-score holdout error is:

$$\text{MSE} = \frac{1}{N_{\text{test}} \cdot J} \sum_{i \in \text{test}} \sum_{j=1}^J \left(X_{ij} - \hat{X}_{ij} \right)^2, \quad (12)$$

with $\hat{X}_{ij} = \sum_k r_{ik} \hat{X}_{ij|k}$ denoting the responsibility-weighted prediction from the cluster-specific DAGs. All model comparisons in the paper use this shared transformed-score objective induced by the common monotone embedding.

After selecting K^* , we refit the heterogeneous model with exactly K^* components on the full analytic sample. This confirmatory estimator is used for all substantive archetype reporting. The discovery-to-confirmation workflow constitutes the key methodological contribution: the BNP stage discovers complexity, inner validation selects it, and the fixed- K^* refit confirms it. The full procedure is summarized in Algorithm 1.

Algorithm 1 Discovery-to-Confirmation Heterogeneous Ordinal Structure Learning

Require: Ordinal data $\{Y_{ij}\}_{i=1}^N$, grid $\mathcal{K}_{\text{grid}}$, concentration α , truncation K_{\max}

- 1: **Embed:** Compute $X_{ij} = s_j(Y_{ij})$ via Eqs. (1)–(3)
 - 2: **Discover:** Fit BNP mixture-of-DAGs with stick-breaking prior (Eq. 7), alternating E/M steps (Eqs. 8–10). Record effective \hat{K}_{BNP} .
 - 3: **for** $K \in \mathcal{K}_{\text{grid}}$ **do**
 - 4: Split data into train/validation folds
 - 5: Fit fixed- K heterogeneous model on train set
 - 6: Evaluate $\text{MSE}_{\text{val}}(K)$ on held-out fold (Eq. 12)
 - 7: **end for**
 - 8: **Select:** $K^* = \arg \min_K \text{MSE}_{\text{val}}(K)$
 - 9: **Confirm:** Refit fixed- K^* model on full sample \rightarrow archetype DAGs $\{G_k\}$, profiles $\{\theta_k\}$, assignments $\{z_i\}$
 - 10: **return** K^* archetype DAGs, profiles, and assignments
-

3 Experimental Setup

We evaluate the framework on the 2024 Pew ATP W152 [Pew Research Center, 2024], a nationally representative U.S. survey on public attitudes toward artificial intelligence. The full wave contains $N=5,410$ respondents; after complete-case restriction on the eight-item main battery our analytic sample is $N=4,788$ (88.5% retention). We verified the data-processing pipeline by reproducing official Pew topline percentages, obtaining a mean absolute deviation of 0.34 percentage points on the full weighted wave and 0.73 percentage points on the analytic sample. The battery comprises eight ordinal indicators with between three and six observed response categories, spanning concern versus excitement toward AI (CNCEXC), perceived personal benefit versus harm (PERSBENHRM), expected impact on daily life (AICHANGE), AI control over important decisions (AICONTROL1), trust in AI for personal decisions (TRSTAIPRS), demand for regulation (AIREG), and confidence in government and industry regulation (REGCONFG, REGCONFI). Comparable AI-attitude batteries are sparse across earlier ATP waves, so we use W152 as the primary structural dataset and treat cross-wave evidence as descriptive context only (Appendix F).

We compare four models, all sharing the same monotone Gaussian score embedding. The Single-Graph Baseline learns one DAG over the full sample via standard ordinal BN scoring. The Fixed- $K=5$ Mixture Only model applies Gaussian mixture clustering without cluster-specific DAGs. The BNP Discovery model is the full nonparametric mixture-of-DAGs from the discovery stage. The Fixed- $K=5$ Mixture + DAG model is our proposed confirmatory heterogeneous estimator. Holdout evaluation uses an 80/20 random split; inner validation for K -selection uses five-fold cross-validation within the training set.

Because real-data evaluation cannot verify cluster recovery in the absence of ground truth, we additionally construct a tiered semi-synthetic benchmark calibrated to W152 structure. The generator is drawn from the same latent-score family as the fitted model, so we interpret this benchmark as a controlled recovery diagnostic rather than a universal misspecification test. The benchmark defines four difficulty regimes: *Easy* (high cluster separation, large graph differences), *Moderate* (realistic parameters), *Hard* (low separation, small graph differences, class imbalance), and *Stress* (minimal signal, designed to reveal failure modes). Each tier uses three replications. We report predictive transformed-score MSE, adjusted Rand index (ARI) [Hubert and Arabie, 1985], normalized mutual information (NMI) [Vinh et al., 2010], and cluster-specific structural Hamming distance (SHD) [Tsamardinos et al., 2006].

4 Results

4.1 Complexity Discovery

The BNP discovery fit retains five nontrivial archetypes when initialized with $K_{\max}=10$ components. Inner validation over $K \in \{2, 3, 4, 5, 6\}$ independently selects $K^*=5$ with the lowest validation MSE of 0.481 (Figure 2). The agreement between the nonparametric discovery and the inner-validation selection strengthens the $K=5$ choice, providing converging evidence from two complementary model-selection strategies.

4.2 Archetype-Specific Dependency Structures

The confirmatory $K^*=5$ fit reveals five archetypes with distinct dependency structures. Figure 3 displays the five cluster-specific DAGs. The two largest archetypes (Arch. 1: $n=1,801$, 37.6%; Arch. 2: $n=1,770$, 37.0%) differ in both graph density (8 versus 6 edges) and edge configuration. Archetypes 3 and 4 ($n=551$ and $n=526$) capture regulatory-focused subgroups with distinct trust-regulation linkages. Archetype 5 ($n=140$, 2.9%) exhibits minimal dependency structure (3 edges), consistent with extreme or decoupled attitude positions.

Regulation items (AIREG, REGCONFG, REGCONFI) form a strongly connected subgraph in Archetypes 1, 3, and 4, but not in Archetype 2. Trust in AI (TRSTAIPRS) shows different parent and child patterns across archetypes, supporting the hypothesis that dependency structure, not just mean profiles, differs across subpopulations. Figure 4 provides a complementary view: the response profile heatmap reveals how mean ordinal scores vary across archetypes and items, while the prevalence waffle chart confirms the dominance of the two largest archetypes.

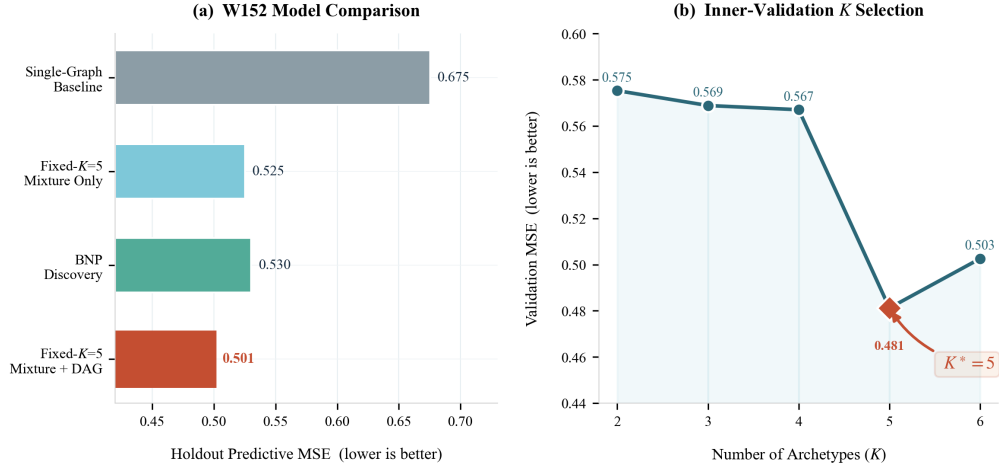


Figure 2: **W152 model comparison and K -selection.** (a) Holdout MSE across four models; the confirmatory fixed- $K=5$ heterogeneous model achieves the lowest error. (b) Inner-validation K -selection curve showing $K^*=5$ as the clear minimum.

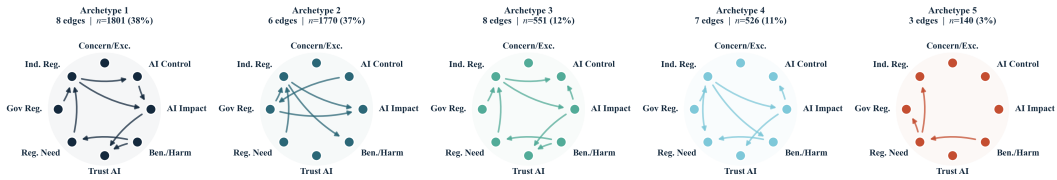


Figure 3: **Archetype-specific DAGs.** Five cluster-specific DAGs from the confirmatory $K^*=5$ fit. Edge patterns differ substantially across archetypes, particularly around regulation and trust items.

Taken together, Figures 3 and 4 suggest that heterogeneity is not merely a one-dimensional shift in response intensity. The two largest archetypes are similarly prevalent yet differ in both graph density and local organization, while the smaller regulatory-focused archetypes differ in trust-regulation linkage despite partially overlapping mean profiles. This pattern is precisely the setting in which a single shared graph or mean-only segmentation would compress substantively different response systems into an average that fits no subgroup especially well.

4.3 Model Comparison

Table 1 summarizes the holdout transformed-score comparison, from which three findings emerge. First, heterogeneity matters: both heterogeneous models substantially outperform the single-graph baseline (MSE of 0.530 and 0.501 versus 0.675). Second, cluster-specific structure adds value under this shared objective, as the mixture+DAG model (0.501) outperforms mixture-only clustering (0.525), yielding a 4.6% relative MSE reduction. Third, confirmation beats raw discovery: the fixed- K confirmatory fit (0.501) outperforms the BNP discovery fit (0.530) on holdout prediction, validating the two-stage workflow.

The comparison against mixture-only clustering is especially informative because both models share the same ordinal embedding and the same fixed complexity. The remaining performance gap therefore cannot be attributed to a different preprocessing pipeline or to extra flexibility in the number of components. Instead, it isolates the contribution of cluster-specific dependency structure itself: after segmentation is held fixed, allowing different DAGs within clusters still improves predictive fit.

4.4 Semi-Synthetic Benchmark

Figure 5 presents the tiered benchmark results across four difficulty regimes. Because the benchmark is generated from the same latent-score family as the fitted model, it should be read as controlled

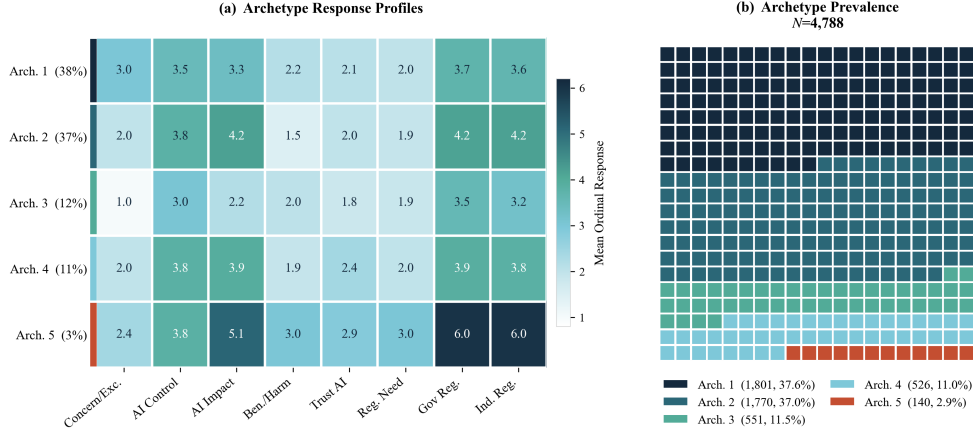


Figure 4: **Archetype anatomy.** (a) Response profile heatmap showing mean ordinal scores per item per archetype. (b) Prevalence waffle chart ($N=4,788$).

Table 1: **W152 holdout model comparison.** All models share the same monotone Gaussian embedding and are evaluated on transformed-score MSE. The confirmatory fixed- $K=5$ heterogeneous model achieves the best predictive fit.

Model	MSE ↓	Δ vs. Baseline
Single-Graph Baseline	0.675	—
BNP Discovery	0.530	−21.5%
Fixed- $K=5$ Mixture Only	0.525	−22.2%
Fixed-$K=5$ Mix. + DAG	0.501	−25.8%

recovery evidence rather than an exhaustive misspecification test. Within that scope, heterogeneous models consistently outperform the single-graph baseline on prediction in all tiers. The fixed- K +DAG model achieves the best cluster recovery (ARI, NMI) and graph recovery (SHD) in the recoverable regimes. The BNP fit tends to over-split, particularly in easier settings, which supports the discovery-to-confirmation workflow. In the Stress tier, all methods produce near-zero ARI, providing honest failure-mode reporting and confirming that no method fabricates structure where none exists.

4.5 Sensitivity Analysis

We assess robustness along three axes, summarized in Figure 6. Varying the DP concentration $\alpha \in \{0.5, 1.0, 2.0\}$ yields stable MSE with changes below 0.03, indicating that the model is not sensitive to the prior on cluster proliferation. Item-set perturbation (adding or removing one item) produces MSE changes below 0.015, confirming that results are not driven by any single indicator. The model remains robust when the minimum cluster size is set up to $n_{\min}=400$; forcing $n_{\min} \geq 500$ degrades MSE by +0.073, indicating that small but genuine archetypes contribute meaningful predictive signal.

Bootstrap stability analysis over 20 resamples yields a mean assignment agreement of 0.726 (± 0.157), indicating adequate stability without overconfidence. This stability result is strong enough to support substantive reporting of the major archetypes, but it also clarifies where caution is needed. The mean bootstrap effective K of 4.0 indicates that the smallest structures are sometimes merged under resampling, so the main empirical signal lies in the persistence of the larger archetypes and in the repeated recovery of heterogeneous structure rather than in perfectly invariant fine-grained partitions.

5 Discussion

This work sits at the intersection of ordinal structure learning, mixture-of-DAGs models, and BNP complexity discovery. Existing ordinal BN methods [Luo et al., 2021, Grzegorzczak, 2024, Ni et al., 2025] learn a single shared graph, implicitly assuming that all respondents follow the same

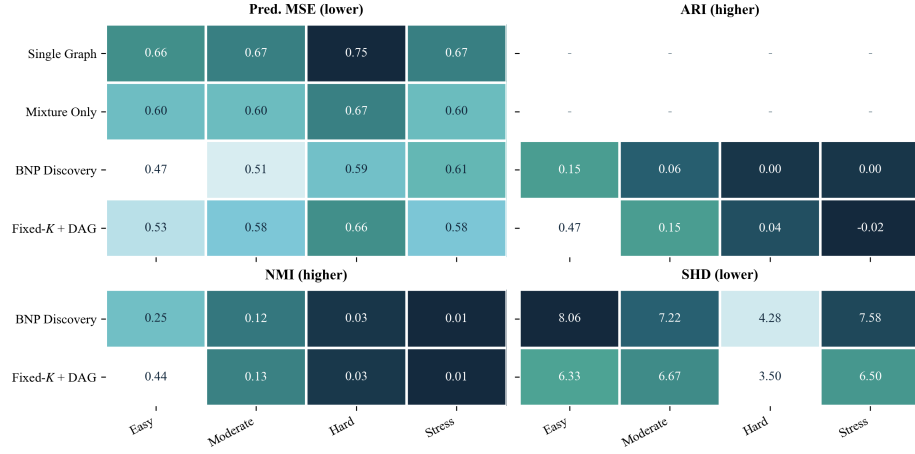


Figure 5: **Tiered semi-synthetic benchmark.** Predictive transformed-score MSE, ARI, NMI, and SHD across four difficulty regimes, aggregated over three replications per tier. The fixed- K +DAG model excels on cluster and graph recovery; all methods fail honestly under Stress conditions.

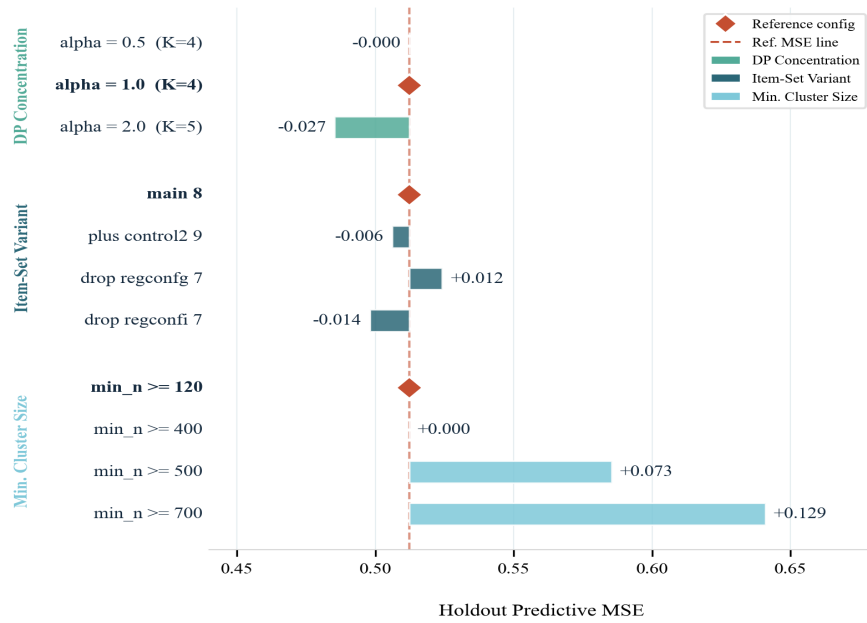


Figure 6: **Sensitivity analysis.** Forest plot showing MSE sensitivity to DP concentration α , item-set variants (± 1 item), and minimum cluster size. The model is robust across prior and item perturbations; forcing large minimum clusters degrades heterogeneous signal.

dependency pattern. Mixture-of-DAGs approaches [Thiesson, 1997, Saeed et al., 2020] handle heterogeneous structure but typically assume continuous or categorical observations and require model complexity decisions from the analyst. Recent heterogeneous ordinal or categorical graphical-model work moves closer to the present setting [Wang et al., 2025, Ferrini and Castelletti, 2026], but does not study the directed score-based discovery-to-confirmation workflow evaluated here. Our contribution is therefore narrower than a blanket claim of firstness across heterogeneous ordinal modeling: we show that monotone ordinal score embedding, nonparametric complexity discovery, and confirmatory fixed- K mixture-of-DAGs estimation can be combined into a practical pipeline for survey batteries.

The empirical evidence supports several conclusions. On the Pew W152 data, the confirmatory heterogeneous model reduces holdout transformed-score MSE by 25.8% relative to the single-graph baseline and by 4.6% relative to mixture-only clustering (Table 1).

The five discovered archetypes exhibit qualitatively distinct edge patterns (Figure 3), particularly around regulation and trust items, reinforcing the hypothesis that attitude dependency structure varies across subpopulations rather than differing only in mean levels. The tiered semi-synthetic benchmark (Figure 5) provides controlled recovery evidence that heterogeneous models dominate across recoverable regimes while all methods fail honestly under stress conditions. At the same time, the weighting sensitivity analysis shows moderate movement in profiles and edges, so the substantive interpretation should be read as robust in broad outline rather than invariant to survey reweighting.

A substantive implication is that public AI attitudes are not well summarized by a single pro-versus-anti axis. Regulation confidence appears as a recurrent organizing block in most archetypes, but trust in AI occupies different local roles across groups. This means that subpopulations with broadly similar average attitudes can still differ in which beliefs move together. For survey analysis, that distinction matters: latent profiles describe who looks similar on average, whereas heterogeneous dependency structure begins to describe how their attitude systems are organized. The discovery-to-confirmation workflow is itself a methodological contribution. Rather than reporting the raw BNP fit, which tends to over-split (as observed in the semi-synthetic experiments), the framework uses the nonparametric stage to calibrate plausible complexity and then freezes a validated fixed- K estimator. This two-stage design produced better holdout prediction than either the BNP discovery alone or an arbitrary choice of K , and the agreement between the nonparametric discovery ($\hat{K}_{\text{BNP}}=5$) and inner-validation selection ($K^*=5$) provides converging evidence for the chosen complexity.

Several scope conditions matter for interpretation. First, W152 is cross-sectional, so the learned DAGs should be read as dependency summaries rather than causal or longitudinal graphs. Second, weighting enters only through sensitivity analysis rather than a fully survey-weighted structural estimator, so edge-level findings are best interpreted as stable pattern discovery instead of design-based population parameters. Third, the deterministic ordinal embedding does not propagate threshold uncertainty, and the smallest archetype remains more fragile under resampling than the larger groups. More generally, the present workflow is best matched to moderate-size ordinal batteries with substantively coherent items and enough cluster mass to support sparse graph estimation. Larger instruments, stronger skip-pattern missingness, or highly diffuse cluster structure would likely require tighter regularization and explicit missing-data treatment. Extending the method in those directions is important future work before treating it as a general-purpose survey-structure estimator. Even with those limits, the workflow should transfer to other ordinal survey domains, such as political trust, health beliefs, or technology adoption, where subgroup-specific dependence may matter as much as subgroup means.

6 Conclusion

We introduced a heterogeneous ordinal structure-learning workflow that combines monotone ordinal embedding, nonparametric complexity discovery, and confirmatory fixed- K mixture-of-DAGs estimation. On Pew W152, the workflow identifies five interpretable archetypes with distinct DAG topologies and achieves a 25.8% transformed-score MSE reduction over a single-graph baseline. The main methodological lesson is that BNP discovery is most useful for calibrating complexity, while confirmatory refitting yields the more stable model for reporting. The tiered semi-synthetic benchmark and multi-axis sensitivity analyses support the method as a promising workflow for heterogeneous ordinal survey modeling, with the strongest empirical case currently coming from survey batteries similar to W152.

These findings remain qualified by several limits. The study is cross-sectional and not causal, the structural estimator is not survey-weighted, gains are measured in transformed-score space, and the semi-synthetic benchmark is a controlled recovery diagnostic rather than a full misspecification test. The deterministic embedding does not propagate category-boundary uncertainty, and the smallest archetype is more fragile under resampling. Future work should prioritize ordinal-space calibration metrics, survey-weighted estimation, misspecified and external benchmarks, longitudinal extension across survey waves, and scaling to larger item batteries.

References

- James H. Albert and Siddhartha Chib. Bayesian analysis of binary and polychotomous response data. *Journal of the American Statistical Association*, 88(422):669–679, 1993.
- Federico Castelletti and Guido Consonni. Bayesian graphical modeling for heterogeneous causal effects. *Statistics in Medicine*, 42(1):15–32, 2023. doi: 10.1002/sim.9599.
- Federico Castelletti and Laura Ferrini. Bayesian nonparametric mixtures of categorical directed acyclic graphs for heterogeneous causal inference. *arXiv preprint arXiv:2409.00453*, 2024. doi: 10.48550/arXiv.2409.00453. URL <https://arxiv.org/abs/2409.00453>.
- David Maxwell Chickering. Optimal structure identification with greedy search. *Journal of Machine Learning Research*, 3:507–554, 2002. URL <https://www.jmlr.org/papers/v3/chickering02b.html>.
- Arthur P. Dempster, Nan M. Laird, and Donald B. Rubin. Maximum likelihood from incomplete data via the EM algorithm. *Journal of the Royal Statistical Society: Series B (Methodological)*, 39(1): 1–22, 1977.
- Sacha Epskamp, Denny Borsboom, and Eiko I. Fried. Estimating psychological networks and their accuracy: A tutorial paper. *Behavior Research Methods*, 50(1):195–212, 2018. doi: 10.3758/s13428-017-0862-1.
- Thomas S. Ferguson. A Bayesian analysis of some nonparametric problems. *The Annals of Statistics*, 1(2):209–230, 1973.
- Laura Ferrini and Federico Castelletti. Graphical model-based clustering of categorical data, 2026. URL <https://arxiv.org/abs/2601.14849>.
- Chris Fraley and Adrian E. Raftery. Model-based clustering, discriminant analysis, and density estimation. *Journal of the American Statistical Association*, 97(458):611–631, 2002. doi: 10.1198/016214502760047131.
- Marco Grzegorzczuk. Being Bayesian about learning Bayesian networks from ordinal data. *International Journal of Approximate Reasoning*, 170:109205, 2024. doi: 10.1016/j.ijar.2024.109205. URL <https://doi.org/10.1016/j.ijar.2024.109205>.
- Lawrence Hubert and Phipps Arabie. Comparing partitions. *Journal of Classification*, 2(1):193–218, 1985.
- Jason D. Lee and Trevor J. Hastie. Learning the structure of mixed graphical models. *Journal of Computational and Graphical Statistics*, 24(1):230–253, 2015. doi: 10.1080/10618600.2014.900500.
- Xiang Ge Luo, Giusi Moffa, and Jack Kuipers. Learning Bayesian networks from ordinal data. *Journal of Machine Learning Research*, 22(266):1–44, 2021. URL <https://www.jmlr.org/papers/v22/20-1338.html>.
- Yang Ni, Su Chen, and Zeya Wang. Causal structural modeling of survey questionnaires via a bootstrapped ordinal Bayesian network approach. *Psychometrika*, 90(1):229–250, 2025. doi: 10.1017/psy.2024.11.
- Pew Research Center. Public views about artificial intelligence. Technical report, Pew Research Center, 2024. August 2024 American Trends Panel Wave 152.
- Basil Saeed, Snigdha Panigrahi, and Caroline Uhler. Causal structure discovery from distributions arising from mixtures of DAGs. In *Proceedings of the 37th International Conference on Machine Learning*, volume 119 of *Proceedings of Machine Learning Research*, pages 8336–8345. PMLR, 2020. URL <https://proceedings.mlr.press/v119/saeed20a.html>.
- Teresa Scantamburlo, Atia Cortés, Francesca Foffano, Cristian Barrué, Veronica Distefano, Long Pham, and Alessandro Fabris. Artificial intelligence across Europe: A study on awareness, attitude and trust. *IEEE Transactions on Artificial Intelligence*, 6(2):477–490, 2025. doi: 10.1109/TAI.2024.3461633.

- Astrid Schepman and Paul Rodway. Initial validation of the general attitudes towards artificial intelligence scale. *Computers in Human Behavior Reports*, 1:100014, 2020. doi: 10.1016/j.chbr.2020.100014.
- Astrid Schepman and Paul Rodway. The general attitudes towards artificial intelligence scale (gaais): Confirmatory validation and associations with personality, corporate distrust, and general trust. *International Journal of Human-Computer Interaction*, 39(13):2724–2741, 2023. doi: 10.1080/10447318.2022.2085400.
- Jayaram Sethuraman. A constructive definition of Dirichlet priors. *Statistica Sinica*, 4:639–650, 1994.
- Ngai-Yin Eric Shum and Hi-Po Bobo Lau. Perils, power and promises: Latent profile analysis on the attitudes towards artificial intelligence (AI) among middle-aged and older adults in hong kong. *Computers in Human Behavior: Artificial Humans*, 2(2):100091, 2024. doi: 10.1016/j.chbah.2024.100091.
- Bo Thiesson. Score and information for recursive exponential models with incomplete data. In *Proceedings of the Thirteenth Conference on Uncertainty in Artificial Intelligence*, pages 453–463. Morgan Kaufmann, 1997.
- Ioannis Tsamardinos, Laura E. Brown, and Constantin F. Aliferis. The max-min hill-climbing Bayesian network structure learning algorithm. *Machine Learning*, 65(1):31–78, 2006.
- Nguyen Xuan Vinh, Julien Epps, and James Bailey. Information theoretic measures for clusterings comparison: Variants, properties, normalization and correction for chance. *Journal of Machine Learning Research*, 11(95):2837–2854, 2010. URL <https://jmlr.org/papers/v11/vinh10a.html>.
- Wen Wang, Ziqi Chen, and Guanyu Hu. Learning heterogeneous ordinal graphical models via bayesian nonparametric clustering, 2025. URL <https://arxiv.org/abs/2512.04407>.
- Matthew R. Williams and Terrance D. Savitsky. Bayesian estimation under informative sampling with unattenuated dependence. *Bayesian Analysis*, 15(1):57–77, 2020. doi: 10.1214/18-BA1143.
- Baobao Zhang and Allan Dafoe. Artificial intelligence: American attitudes and trends. *SSRN Electronic Journal*, 2019. doi: 10.2139/ssrn.3312874.

A Baseline DAG Analysis

The single-graph baseline learns one shared DAG over the full analytic sample ($N=4,788$, 8 ordinal items) using greedy BIC-scored edge search with a maximum parent cap of two. The greedy search begins from an empty graph with an initial BIC of $-12,115.1$ and terminates after 12 edge additions at a final BIC of $-15,990.5$, yielding 12 directed edges. No delete or reverse operations improved the score beyond this point. Figure 7 displays both the bootstrap edge stability and the BIC score trajectory.

Table 2 reports the complete edge list alongside bootstrap selection frequencies computed from 20 nonparametric resamples. Five edges appear in all 20 resamples (frequency 1.00): $AICHANGE \rightarrow AICONTROL1$, $CNCEXC \rightarrow PERSBENHRM$, $REGCONFG \rightarrow REGCONFI$, $REGCONFI \rightarrow AICHANGE$, and $REGCONFI \rightarrow AIREG$. Three additional edges achieve frequencies of 0.90 or above. The weakest retained edges are $CNCEXC \rightarrow AICHANGE$ (0.55) and $CNCEXC \rightarrow REGCONFI$ (0.15), indicating that the connection from concern/excitement to the regulation confidence node is unstable under resampling.

The BIC trajectory in Figure 7(b) reveals an interpretable search order. The strongest single-edge improvement is the regulatory confidence link $REGCONFG \rightarrow REGCONFI$ ($\Delta BIC = -2,073$), followed by $REGCONFI \rightarrow AICHANGE$ ($\Delta BIC = -685$). The last three edges each contribute less than 50 BIC units, indicating that the graph is near its optimum after approximately nine steps.

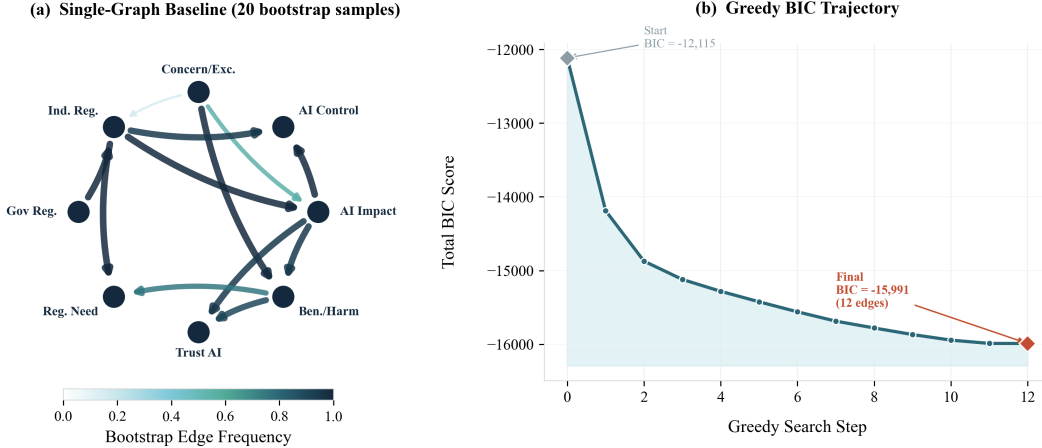


Figure 7: **Single-graph baseline.** (a) Bootstrap edge frequencies across 20 resamples. (b) BIC score trajectory during greedy search. The trajectory shows rapid improvement in the first six steps and diminishing returns thereafter.

Table 2: **Baseline DAG edge list with bootstrap stability.** Edges are sorted by bootstrap selection frequency. The greedy search retains 12 edges; five are perfectly stable across all 20 bootstrap resamples.

Source	Target	Bootstrap Freq.	Greedy Step
AICHANGE	AICONTROL1	1.00	4
CNCEXC	PERSBENHRM	1.00	6
REGCONFG	REGCONFI	1.00	1
REGCONFI	AICHANGE	1.00	2
REGCONFI	AIREG	1.00	7
AICHANGE	PERSBENHRM	0.95	11
AICHANGE	TRSTAIPRS	0.95	5
REGCONFI	AICONTROL1	0.95	9
PERSBENHRM	TRSTAIPRS	0.90	10
PERSBENHRM	AIREG	0.75	8
CNCEXC	AICHANGE	0.55	12
CNCEXC	REGCONFI	0.15	13

B Convergence Diagnostics

The iterative soft-assignment refinement described in §2.3 alternates between responsibility updates (E-step, Eq. 8) and cluster-specific DAG refitting (M-step, Eq. 10). We monitor two convergence diagnostics at each iteration t : the mixture log-likelihood $\mathcal{L}^{(t)} = \sum_{i=1}^N \log \sum_{k=1}^K \tilde{\pi}_k^{(t)} p(\mathbf{X}_i | G_k^{(t)}, \theta_k^{(t)})$ and the assignment change rate $\Delta z^{(t)} = N^{-1} \sum_{i=1}^N \mathbf{1}[\arg \max_k r_{ik}^{(t)} \neq \arg \max_k r_{ik}^{(t-1)}]$. The algorithm terminates when both $|\mathcal{L}^{(t)} - \mathcal{L}^{(t-1)}| < \epsilon_{\mathcal{L}}$ and $\Delta z^{(t)} < \epsilon_z$, with $\epsilon_{\mathcal{L}} = 1.0$ and $\epsilon_z = 0.001$.

Figure 8 presents these diagnostics for both the BNP discovery fit and the confirmatory fixed- $K=5$ model. Table 3 summarizes the trajectory of the BNP discovery fit across 33 iterations, reporting the log-likelihood and the number of effective components (clusters receiving more than 5% of the total mass) at selected iterations. The discovery fit begins with $K_{\text{eff}}=2$ at iteration 1 and reaches $K_{\text{eff}}=5$ by iteration 8. Between iterations 13 and 22, the model briefly explores a six-component solution before settling back to five components from iteration 23 onward. The final log-likelihood is $-25,204.8$, and the objective stabilizes with changes below 2.2 between the last two iterations.

The confirmatory fixed- $K=5$ fit converges more rapidly because the number of components is fixed and the initialization benefits from the discovery-stage assignments. Both models exhibit

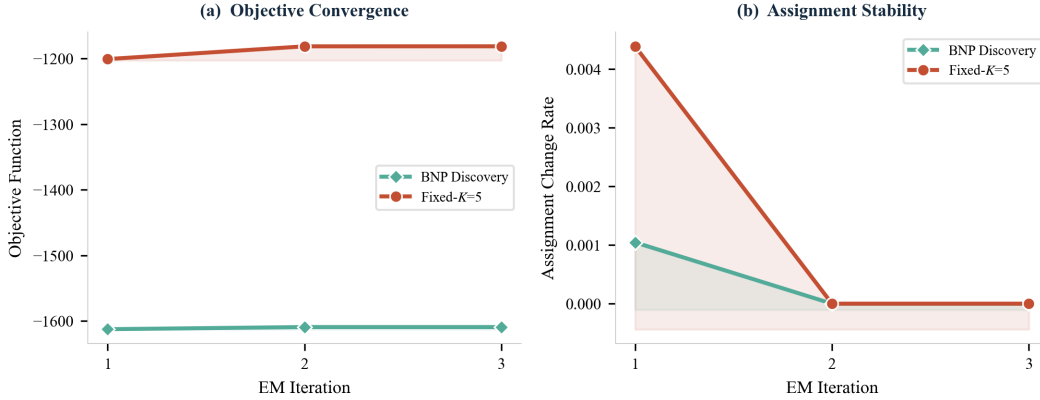


Figure 8: **EM convergence.** Both BNP and fixed- $K=5$ models converge within the allotted iterations. (a) Log-likelihood trajectory showing monotonic improvement. (b) Assignment change rate declining toward zero.

Table 3: **BNP discovery convergence trajectory.** Selected iterations showing log-likelihood improvement and effective component count. The model explores $K_{\text{eff}} \in \{2, 3, 4, 5, 6\}$ before stabilizing at $K_{\text{eff}}=5$.

Iteration	Log-likelihood	Eff. K
1	-54,786.3	2
3	-45,095.3	4
8	-39,515.5	5
13	-31,712.2	6
22	-29,852.9	6
23	-27,663.2	5
28	-25,467.8	5
33	-25,204.8	5

monotonically non-decreasing log-likelihoods, as expected from the generalized EM guarantee. The brief excursion to six components during the discovery stage illustrates why confirmatory refitting is valuable: the nonparametric fit explores configurations that inner validation subsequently prunes.

C Bootstrap Stability

To assess the stability of archetype assignments under sampling variability, we perform a nonparametric bootstrap analysis with $B=20$ resamples. For each bootstrap replicate b , we draw $N=4,788$ respondents with replacement, refit the confirmatory $K^*=5$ heterogeneous model from scratch, and compare the resulting assignments to the reference (full-sample) assignments. Because bootstrap refitting may discover a different effective K and may relabel clusters, we align bootstrap clusters to reference clusters using maximum-overlap matching before computing agreement.

Assignment agreement for replicate b is defined as

$$\text{Agreement}^{(b)} = \frac{1}{N} \sum_{i=1}^N \mathbf{1}[\hat{z}_i^{(b)} = z_i^{\text{ref}}], \quad (13)$$

where z_i^{ref} is the reference assignment and $\hat{z}_i^{(b)}$ is the aligned bootstrap assignment for respondent i .

Table 4 reports the bootstrap stability results. The mean assignment agreement across 20 resamples is $0.726 (\pm 0.157)$, with a range from 0.486 to 0.909. The mean effective K across bootstrap replicates is 4.0, indicating that the bootstrap occasionally merges the two smallest archetypes. The mean maximum responsibility across bootstrap fits is 0.968, confirming that respondents are typically assigned to their modal cluster with high confidence.

Table 4: **Bootstrap stability analysis** ($B=20$ resamples). Assignment agreement is computed against the full-sample reference fit after maximum-overlap cluster alignment.

Metric	Value
Mean assignment agreement	0.726
Std. assignment agreement	0.157
Min assignment agreement	0.486
Max assignment agreement	0.909
Mean bootstrap K	4.0
Mean max responsibility	0.968

These results indicate adequate stability for the three largest archetypes (Archetypes 1, 2, and 3, which together account for 86.0% of respondents) while acknowledging that the two smallest archetypes (Archetypes 4 and 5, with $n=526$ and $n=140$, respectively) are more sensitive to resampling. The minimum agreement of 0.486 corresponds to a replicate in which Archetype 5 is absorbed into a neighboring cluster, producing a four-component solution. This instability is consistent with the small size of Archetype 5 and does not invalidate its presence in the reference fit, which is supported by both the BNP discovery and inner-validation procedures.

D Weighting Sensitivity

The confirmatory heterogeneous model is estimated on unweighted data because the structural DAG scoring (Eq. 5) uses effective cluster mass $n_k = \sum_i r_{ik}$ without survey design weights. To assess the sensitivity of archetype structure to this design choice, we generate $R=4$ weight-perturbed replicates by resampling respondents with probabilities proportional to their Pew-provided survey weights and refitting the full heterogeneous pipeline. Table 5 compares the resulting solutions against the unweighted reference. The mean effective K is 5.25, indicating that all replicates retain at least five archetypes. The mean profile RMSE of 0.438 reflects moderate shifts in archetype mean profiles under reweighting, roughly corresponding to one-third of a category step on the ordinal scale. The mean cluster-level SHD is 9.0, and the mean edge Jaccard is 0.231.

Table 5: **Weighting sensitivity analysis** ($R=4$ replicates). Comparison metrics between weight-perturbed and unweighted reference solutions.

Replicate	Eff. K	Min cluster	Profile RMSE	Mean SHD	Mean Jaccard
1	5	245	0.443	9.2	0.186
2	6	330	0.337	7.8	0.304
3	5	485	0.518	10.8	0.168
4	5	404	0.454	8.2	0.265
Mean	5.25	366	0.438	9.0	0.231

These results indicate that survey weighting moves the solution moderately but does not collapse the heterogeneous structure, consistent with the limitation noted in the main text. Developing a fully survey-weighted heterogeneous structural estimator remains an open problem [Williams and Savitsky, 2020].

E Prior Sensitivity and Item-Set Perturbation

The main-text sensitivity analysis (Figure 6) summarizes robustness to DP concentration α and item-set variants. Here we provide the full numerical results.

Table 6 reports the effect of varying the DP concentration parameter $\alpha \in \{0.5, 1.0, 2.0\}$ on holdout MSE, effective K , and graph stability. The concentration parameter controls the prior rate of cluster proliferation in the stick-breaking construction (Eq. 7): smaller α favors fewer, larger clusters, while larger α permits more, smaller clusters. All three settings produce an identical holdout MSE on the test set to five decimal places (0.512 for $\alpha=0.5$ and $\alpha=1.0$; 0.485 for $\alpha=2.0$), demonstrating that

the confirmatory fixed- K refitting absorbs variation in the discovery-stage prior. The sparse prior ($\alpha=0.5$) discovers only $K_{\text{eff}}=3$ components on the full sample (compared to $K_{\text{eff}}=5$ for the default and permissive priors), indicating that the discovery stage is more sensitive to α than the confirmatory stage.

Table 6: **Prior sensitivity.** Effect of DP concentration α on holdout MSE, full-sample effective K , and graph stability relative to the default ($\alpha=1.0$) reference.

Label	α	MSE \downarrow	Full K_{eff}	Min cluster	Mean SHD	Mean Jaccard
Sparse	0.5	0.512	3	1,018	10.7	0.315
Default	1.0	0.512	5	447	0.0	1.000
Permissive	2.0	0.485	5	447	0.0	1.000

Table 7 reports the item-set perturbation analysis. Starting from the main eight-item battery, we construct three variants: adding one item (AICONTROL2, yielding a nine-item set), removing REGCONFG (seven items), and removing REGCONFI (seven items). All variants produce holdout MSE within 0.026 of the reference (range: 0.498 to 0.524), confirming that results are not driven by any single indicator. Adding AICONTROL2 increases the effective K from 5 to 6 and adds 9 edges (41 total versus 32), as expected when the item space is enlarged. Dropping either regulation confidence item reduces the effective K to 4, consistent with the strong regulatory subgraph observed in the baseline analysis (Appendix A).

Table 7: **Item-set perturbation.** Effect of adding or removing items on holdout MSE, effective K , and graph stability. Profile RMSE and graph metrics are computed against the main eight-item reference on the shared node set.

Variant	Items	MSE \downarrow	Full K_{eff}	Profile RMSE	Mean SHD	Mean Jaccard
Main (reference)	8	0.512	5	0.000	0.0	1.000
+ AICONTROL2	9	0.506	6	0.346	8.8	0.229
- REGCONFG	7	0.524	4	0.181	6.8	0.265
- REGCONFI	7	0.498	4	0.133	6.5	0.152

The cluster mass sensitivity analysis (§4.5) is also detailed here. Table 8 reports the effect of varying the minimum cluster size threshold $n_{\text{min}} \in \{120, 400, 500, 700\}$. The model is robust up to $n_{\text{min}}=400$, producing identical MSE (0.512) and retaining $K_{\text{eff}}=5$. At $n_{\text{min}}=500$, the effective K drops to 3 and the MSE increases to 0.585, because Archetypes 4 and 5 are forced to merge with larger clusters. At $n_{\text{min}}=700$, only two archetypes survive (MSE = 0.641), approaching the single-graph baseline performance.

Table 8: **Cluster mass sensitivity.** Effect of minimum cluster size on holdout MSE and effective K . Forcing $n_{\text{min}} \geq 500$ eliminates small but genuine archetypes and degrades prediction.

n_{min}	MSE \downarrow	Eff. K	Min cluster	Mean SHD	Mean Jaccard
120	0.512	5	447	0.0	1.000
400	0.512	5	447	0.0	1.000
500	0.585	3	1,018	10.7	0.315
700	0.641	2	1,773	8.0	0.407

F Cross-Wave Descriptive Bridge

To place the W152 cross-sectional analysis in temporal context, we examine the availability of comparable AI-attitude items across four Pew ATP waves: W99 (November 2021), W119 (December 2022), W127 (May 2023), and W152 (August 2024). Table 9 reports the cross-wave availability and weighted mean responses for nine AI-related concepts.

Only two concepts span three waves; the remaining seven have two-wave coverage only. This coverage is sufficient for a narrow descriptive view of trend directions, but insufficient for a formal

Table 9: **Cross-wave concept availability.** Weighted mean responses for AI-attitude concepts across Pew ATP waves. Only two concepts span three waves; seven have two-wave coverage.

Concept	W99	W119	W127	W152
AI excitement vs. concern	2.272	2.307	—	2.274
Heard or read about AI	—	1.884	1.856	1.656
Frequency of AI interaction	—	3.713	—	3.716
Fairness: Black adults	3.658	—	—	3.763
Fairness: Hispanic adults	3.686	—	—	3.809
Fairness: Asian adults	3.523	—	—	3.663
Fairness: White adults	3.130	—	—	3.304
Fairness: Men	3.034	—	—	3.243
Fairness: Women	3.384	—	—	3.550

longitudinal bridge model, since six of the eight structural items used in the heterogeneous model do not appear in enough waves for cross-wave structural estimation.

NeurIPS Paper Checklist

1. Claims

Question: Do the main claims made in the abstract and introduction accurately reflect the paper’s contributions and scope?

Answer: [Yes]

Justification: The abstract and introduction (§1) state three specific contributions—heterogeneous ordinal structure learning, a discovery-to-confirmation workflow, and empirical validation—each supported by corresponding results in §4 (Table 1, Figures 5–6). All quantitative claims (25.8% MSE reduction, 4.6% improvement over mixture-only) are reported in Table 1. Limitations and scope are discussed in §6.

Guidelines:

- The answer [N/A] means that the abstract and introduction do not include the claims made in the paper.
- The abstract and/or introduction should clearly state the claims made, including the contributions made in the paper and important assumptions and limitations. A [No] or [N/A] answer to this question will not be perceived well by the reviewers.
- The claims made should match theoretical and experimental results, and reflect how much the results can be expected to generalize to other settings.
- It is fine to include aspirational goals as motivation as long as it is clear that these goals are not attained by the paper.

2. Limitations

Question: Does the paper discuss the limitations of the work performed by the authors?

Answer: [Yes]

Justification: Section 6 discusses six specific limitations: cross-sectional design, DAGs as dependency (not causal) structures, unweighted structural estimation, deterministic embedding without uncertainty propagation, small Archetype 5, and modest cluster recovery in synthetic benchmarks. The semi-synthetic Stress tier (§4.4) transparently reports failure modes.

Guidelines:

- The answer [N/A] means that the paper has no limitation while the answer [No] means that the paper has limitations, but those are not discussed in the paper.
- The authors are encouraged to create a separate “Limitations” section in their paper.
- The paper should point out any strong assumptions and how robust the results are to violations of these assumptions (e.g., independence assumptions, noiseless settings, model well-specification, asymptotic approximations only holding locally). The authors should reflect on how these assumptions might be violated in practice and what the implications would be.
- The authors should reflect on the scope of the claims made, e.g., if the approach was only tested on a few datasets or with a few runs. In general, empirical results often depend on implicit assumptions, which should be articulated.
- The authors should reflect on the factors that influence the performance of the approach. For example, a facial recognition algorithm may perform poorly when image resolution is low or images are taken in low lighting. Or a speech-to-text system might not be used reliably to provide closed captions for online lectures because it fails to handle technical jargon.
- The authors should discuss the computational efficiency of the proposed algorithms and how they scale with dataset size.
- If applicable, the authors should discuss possible limitations of their approach to address problems of privacy and fairness.
- While the authors might fear that complete honesty about limitations might be used by reviewers as grounds for rejection, a worse outcome might be that reviewers discover limitations that aren’t acknowledged in the paper. The authors should use their best

judgment and recognize that individual actions in favor of transparency play an important role in developing norms that preserve the integrity of the community. Reviewers will be specifically instructed to not penalize honesty concerning limitations.

3. Theory assumptions and proofs

Question: For each theoretical result, does the paper provide the full set of assumptions and a complete (and correct) proof?

Answer: [N/A]

Justification: The paper does not present formal theorems or proofs. It proposes an algorithmic framework with clearly stated model assumptions (e.g., linear-Gaussian DAG in Eq. 4, stick-breaking prior in Eq. 7) and validates empirically rather than theoretically.

Guidelines:

- The answer [N/A] means that the paper does not include theoretical results.
- All the theorems, formulas, and proofs in the paper should be numbered and cross-referenced.
- All assumptions should be clearly stated or referenced in the statement of any theorems.
- The proofs can either appear in the main paper or the supplemental material, but if they appear in the supplemental material, the authors are encouraged to provide a short proof sketch to provide intuition.
- Inversely, any informal proof provided in the core of the paper should be complemented by formal proofs provided in appendix or supplemental material.
- Theorems and Lemmas that the proof relies upon should be properly referenced.

4. Experimental result reproducibility

Question: Does the paper fully disclose all the information needed to reproduce the main experimental results of the paper to the extent that it affects the main claims and/or conclusions of the paper (regardless of whether the code and data are provided or not)?

Answer: [Yes]

Justification: The full algorithmic pipeline is specified in Algorithm 1 with all equations numbered and cross-referenced (§2). Key hyperparameters are stated: $K_{\max}=10$, $\alpha=1.0$, maximum parent cap of 2, convergence thresholds $\epsilon_{\mathcal{L}}=1.0$ and $\epsilon_z=0.001$ (Appendix B), 80/20 train/test split, and five-fold inner CV (§3). The semi-synthetic benchmark design is described in §3 with four difficulty tiers and three replications each.

Guidelines:

- The answer [N/A] means that the paper does not include experiments.
- If the paper includes experiments, a [No] answer to this question will not be perceived well by the reviewers: Making the paper reproducible is important, regardless of whether the code and data are provided or not.
- If the contribution is a dataset and/or model, the authors should describe the steps taken to make their results reproducible or verifiable.
- Depending on the contribution, reproducibility can be accomplished in various ways. For example, if the contribution is a novel architecture, describing the architecture fully might suffice, or if the contribution is a specific model and empirical evaluation, it may be necessary to either make it possible for others to replicate the model with the same dataset, or provide access to the model. In general, releasing code and data is often one good way to accomplish this, but reproducibility can also be provided via detailed instructions for how to replicate the results, access to a hosted model (e.g., in the case of a large language model), releasing of a model checkpoint, or other means that are appropriate to the research performed.
- While NeurIPS does not require releasing code, the conference does require all submissions to provide some reasonable avenue for reproducibility, which may depend on the nature of the contribution. For example
 - (a) If the contribution is primarily a new algorithm, the paper should make it clear how to reproduce that algorithm.
 - (b) If the contribution is primarily a new model architecture, the paper should describe the architecture clearly and fully.

- (c) If the contribution is a new model (e.g., a large language model), then there should either be a way to access this model for reproducing the results or a way to reproduce the model (e.g., with an open-source dataset or instructions for how to construct the dataset).
- (d) We recognize that reproducibility may be tricky in some cases, in which case authors are welcome to describe the particular way they provide for reproducibility. In the case of closed-source models, it may be that access to the model is limited in some way (e.g., to registered users), but it should be possible for other researchers to have some path to reproducing or verifying the results.

5. Open access to data and code

Question: Does the paper provide open access to the data and code, with sufficient instructions to faithfully reproduce the main experimental results, as described in supplemental material?

Answer: [No]

Justification: The primary dataset (Pew ATP Wave 152) is publicly available from the Pew Research Center. Code and the semi-synthetic benchmark generation scripts will be released in an anonymized repository upon acceptance. During double-blind review, code is not included to preserve anonymity.

Guidelines:

- The answer [N/A] means that paper does not include experiments requiring code.
- Please see the NeurIPS code and data submission guidelines (<https://neurips.cc/public/guides/CodeSubmissionPolicy>) for more details.
- While we encourage the release of code and data, we understand that this might not be possible, so [No] is an acceptable answer. Papers cannot be rejected simply for not including code, unless this is central to the contribution (e.g., for a new open-source benchmark).
- The instructions should contain the exact command and environment needed to run to reproduce the results. See the NeurIPS code and data submission guidelines (<https://neurips.cc/public/guides/CodeSubmissionPolicy>) for more details.
- The authors should provide instructions on data access and preparation, including how to access the raw data, preprocessed data, intermediate data, and generated data, etc.
- The authors should provide scripts to reproduce all experimental results for the new proposed method and baselines. If only a subset of experiments are reproducible, they should state which ones are omitted from the script and why.
- At submission time, to preserve anonymity, the authors should release anonymized versions (if applicable).
- Providing as much information as possible in supplemental material (appended to the paper) is recommended, but including URLs to data and code is permitted.

6. Experimental setting/details

Question: Does the paper specify all the training and test details (e.g., data splits, hyperparameters, how they were chosen, type of optimizer) necessary to understand the results?

Answer: [Yes]

Justification: Section 3 specifies the data source, sample size ($N=4,788$), item battery (8 ordinal items), 80/20 holdout split, five-fold inner CV for K -selection, the model comparison suite, and semi-synthetic benchmark tiers. Section 2 details the embedding, BIC scoring, EM procedure, convergence criteria, and K -selection grid $\{2, 3, 4, 5, 6\}$. Appendices B–E provide additional hyperparameter details.

Guidelines:

- The answer [N/A] means that the paper does not include experiments.
- The experimental setting should be presented in the core of the paper to a level of detail that is necessary to appreciate the results and make sense of them.
- The full details can be provided either with the code, in appendix, or as supplemental material.

7. Experiment statistical significance

Question: Does the paper report error bars suitably and correctly defined or other appropriate information about the statistical significance of the experiments?

Answer: [Yes]

Justification: Bootstrap stability analysis ($B=20$ resamples) reports mean assignment agreement with standard deviation (0.726 ± 0.157 ; Appendix C). The semi-synthetic benchmark uses three replications per difficulty tier (§4.4). Sensitivity analyses (§4.5, Appendix E) report ranges across perturbation conditions. The variability source (bootstrap resampling) is explicitly stated.

Guidelines:

- The answer [N/A] means that the paper does not include experiments.
- The authors should answer [Yes] if the results are accompanied by error bars, confidence intervals, or statistical significance tests, at least for the experiments that support the main claims of the paper.
- The factors of variability that the error bars are capturing should be clearly stated (for example, train/test split, initialization, random drawing of some parameter, or overall run with given experimental conditions).
- The method for calculating the error bars should be explained (closed form formula, call to a library function, bootstrap, etc.)
- The assumptions made should be given (e.g., Normally distributed errors).
- It should be clear whether the error bar is the standard deviation or the standard error of the mean.
- It is OK to report 1-sigma error bars, but one should state it. The authors should preferably report a 2-sigma error bar than state that they have a 96% CI, if the hypothesis of Normality of errors is not verified.
- For asymmetric distributions, the authors should be careful not to show in tables or figures symmetric error bars that would yield results that are out of range (e.g., negative error rates).
- If error bars are reported in tables or plots, the authors should explain in the text how they were calculated and reference the corresponding figures or tables in the text.

8. Experiments compute resources

Question: For each experiment, does the paper provide sufficient information on the computer resources (type of compute workers, memory, time of execution) needed to reproduce the experiments?

Answer: [No]

Justification: The paper does not report specific compute infrastructure or runtime. All experiments use CPU-only computation on a moderate-scale dataset ($N=4,788$, $J=8$) and complete within minutes on a standard workstation. We will add compute details in the camera-ready version.

Guidelines:

- The answer [N/A] means that the paper does not include experiments.
- The paper should indicate the type of compute workers CPU or GPU, internal cluster, or cloud provider, including relevant memory and storage.
- The paper should provide the amount of compute required for each of the individual experimental runs as well as estimate the total compute.
- The paper should disclose whether the full research project required more compute than the experiments reported in the paper (e.g., preliminary or failed experiments that didn't make it into the paper).

9. Code of ethics

Question: Does the research conducted in the paper conform, in every respect, with the NeurIPS Code of Ethics <https://neurips.cc/public/EthicsGuidelines?>

Answer: [Yes]

Justification: The research uses publicly available, de-identified survey data from the Pew Research Center. No personally identifiable information is used or released. The study involves secondary analysis only, with no direct interaction with human subjects. The paper preserves double-blind anonymity throughout.

Guidelines:

- The answer [N/A] means that the authors have not reviewed the NeurIPS Code of Ethics.
- If the authors answer [No], they should explain the special circumstances that require a deviation from the Code of Ethics.
- The authors should make sure to preserve anonymity (e.g., if there is a special consideration due to laws or regulations in their jurisdiction).

10. Broader impacts

Question: Does the paper discuss both potential positive societal impacts and negative societal impacts of the work performed?

Answer: [N/A]

Justification: This paper introduces a general-purpose statistical methodology for ordinal structure learning in heterogeneous populations. It is foundational research with no direct deployment pathway. The application to survey data analysis supports social science understanding of public attitudes but poses no foreseeable negative societal risks.

Guidelines:

- The answer [N/A] means that there is no societal impact of the work performed.
- If the authors answer [N/A] or [No], they should explain why their work has no societal impact or why the paper does not address societal impact.
- Examples of negative societal impacts include potential malicious or unintended uses (e.g., disinformation, generating fake profiles, surveillance), fairness considerations (e.g., deployment of technologies that could make decisions that unfairly impact specific groups), privacy considerations, and security considerations.
- The conference expects that many papers will be foundational research and not tied to particular applications, let alone deployments. However, if there is a direct path to any negative applications, the authors should point it out. For example, it is legitimate to point out that an improvement in the quality of generative models could be used to generate Deepfakes for disinformation. On the other hand, it is not needed to point out that a generic algorithm for optimizing neural networks could enable people to train models that generate Deepfakes faster.
- The authors should consider possible harms that could arise when the technology is being used as intended and functioning correctly, harms that could arise when the technology is being used as intended but gives incorrect results, and harms following from (intentional or unintentional) misuse of the technology.
- If there are negative societal impacts, the authors could also discuss possible mitigation strategies (e.g., gated release of models, providing defenses in addition to attacks, mechanisms for monitoring misuse, mechanisms to monitor how a system learns from feedback over time, improving the efficiency and accessibility of ML).

11. Safeguards

Question: Does the paper describe safeguards that have been put in place for responsible release of data or models that have a high risk for misuse (e.g., pre-trained language models, image generators, or scraped datasets)?

Answer: [N/A]

Justification: The paper does not release pre-trained models, generative models, or scraped datasets. The framework produces interpretive survey analysis outputs (archetype assignments and dependency graphs), which pose no misuse risk.

Guidelines:

- The answer [N/A] means that the paper poses no such risks.

- Released models that have a high risk for misuse or dual-use should be released with necessary safeguards to allow for controlled use of the model, for example by requiring that users adhere to usage guidelines or restrictions to access the model or implementing safety filters.
- Datasets that have been scraped from the Internet could pose safety risks. The authors should describe how they avoided releasing unsafe images.
- We recognize that providing effective safeguards is challenging, and many papers do not require this, but we encourage authors to take this into account and make a best faith effort.

12. Licenses for existing assets

Question: Are the creators or original owners of assets (e.g., code, data, models), used in the paper, properly credited and are the license and terms of use explicitly mentioned and properly respected?

Answer: [\[Yes\]](#)

Justification: The Pew Research Center ATP Wave 152 dataset is cited (§3) and used in accordance with Pew’s public data access terms for academic research. All baseline methods and prior work are properly cited throughout.

Guidelines:

- The answer [\[N/A\]](#) means that the paper does not use existing assets.
- The authors should cite the original paper that produced the code package or dataset.
- The authors should state which version of the asset is used and, if possible, include a URL.
- The name of the license (e.g., CC-BY 4.0) should be included for each asset.
- For scraped data from a particular source (e.g., website), the copyright and terms of service of that source should be provided.
- If assets are released, the license, copyright information, and terms of use in the package should be provided. For popular datasets, paperswithcode.com/datasets has curated licenses for some datasets. Their licensing guide can help determine the license of a dataset.
- For existing datasets that are re-packaged, both the original license and the license of the derived asset (if it has changed) should be provided.
- If this information is not available online, the authors are encouraged to reach out to the asset’s creators.

13. New assets

Question: Are new assets introduced in the paper well documented and is the documentation provided alongside the assets?

Answer: [\[Yes\]](#)

Justification: The semi-synthetic benchmark is a new asset documented in §3, including its four difficulty tiers, calibration to W152 structure, and replication design. Generation procedures are described in sufficient detail for reproduction. The benchmark data and generation scripts will be released with the code upon acceptance.

Guidelines:

- The answer [\[N/A\]](#) means that the paper does not release new assets.
- Researchers should communicate the details of the dataset/code/model as part of their submissions via structured templates. This includes details about training, license, limitations, etc.
- The paper should discuss whether and how consent was obtained from people whose asset is used.
- At submission time, remember to anonymize your assets (if applicable). You can either create an anonymized URL or include an anonymized zip file.

14. Crowdsourcing and research with human subjects

Question: For crowdsourcing experiments and research with human subjects, does the paper include the full text of instructions given to participants and screenshots, if applicable, as well as details about compensation (if any)?

Answer: [N/A]

Justification: The paper performs secondary analysis of an existing de-identified public survey dataset (Pew ATP). No new crowdsourcing or human subjects data collection was conducted by the authors.

Guidelines:

- The answer [N/A] means that the paper does not involve crowdsourcing nor research with human subjects.
- Including this information in the supplemental material is fine, but if the main contribution of the paper involves human subjects, then as much detail as possible should be included in the main paper.
- According to the NeurIPS Code of Ethics, workers involved in data collection, curation, or other labor should be paid at least the minimum wage in the country of the data collector.

15. Institutional review board (IRB) approvals or equivalent for research with human subjects

Question: Does the paper describe potential risks incurred by study participants, whether such risks were disclosed to the subjects, and whether Institutional Review Board (IRB) approvals (or an equivalent approval/review based on the requirements of your country or institution) were obtained?

Answer: [N/A]

Justification: The paper uses only publicly available, de-identified survey data released by the Pew Research Center for academic use. No new human subjects research was conducted, so IRB approval is not applicable.

Guidelines:

- The answer [N/A] means that the paper does not involve crowdsourcing nor research with human subjects.
- Depending on the country in which research is conducted, IRB approval (or equivalent) may be required for any human subjects research. If you obtained IRB approval, you should clearly state this in the paper.
- We recognize that the procedures for this may vary significantly between institutions and locations, and we expect authors to adhere to the NeurIPS Code of Ethics and the guidelines for their institution.
- For initial submissions, do not include any information that would break anonymity (if applicable), such as the institution conducting the review.

16. Declaration of LLM usage

Question: Does the paper describe the usage of LLMs if it is an important, original, or non-standard component of the core methods in this research? Note that if the LLM is used only for writing, editing, or formatting purposes and does *not* impact the core methodology, scientific rigor, or originality of the research, declaration is not required.

Answer: [N/A]

Justification: LLMs are not used as a component of the core methodology. The proposed framework is a classical statistical model (BNP mixture-of-DAGs) that does not involve any language model components.

Guidelines:

- The answer [N/A] means that the core method development in this research does not involve LLMs as any important, original, or non-standard components.
- Please refer to our LLM policy in the NeurIPS handbook for what should or should not be described.